

1 **New insights into the manual activities of individuals from the Phaleron**
2 **cemetery (Archaic Athens, Greece)**

3

4 Karakostis Fotios Alexandros^{1,2*}, Buikstra Jane E.^{3,4}, Prevedorou Eleanna^{3,4},
5 Hannigan Elizabeth M⁵, Hotaling Jessica⁵, Hotz Gerhard⁶, Liedl Hannah⁷, Moraitis
6 Konstantinos⁸, Siek Thomas J⁴, Waltenberger Lukas^{9,10}, Widrick Kerri J⁴, Harvati,
7 Katerina^{1,2}

8

9 ¹Paleoanthropology, Senckenberg Centre for Human Evolution and
10 Palaeoenvironment, Institute of Archaeological Sciences, University of Tübingen,
11 Tübingen 72070, Germany.

12 ²DFG (Deutsche Forschungsgemeinschaft) Center for Advanced Studies “Words,
13 Bones, Genes, Tools”, University of Tübingen, Tübingen 72070, Germany.

14 ³Center for Bioarchaeological Research, School of Human Evolution and Social
15 Change, Arizona State University, Tempe, Arizona 85281, United States.

16 ⁴Malcolm H. Wiener Laboratory of Archaeological Science, American School of
17 Classical Studies at Athens, Athens 10676, Greece.

18 ⁵Department of Anthropology, California State University, Chico, California 95929–
19 0400, United States.

20 ⁶Anthropological Collection, Natural History Museum of Basel, Basel 4051,
21 Switzerland.

22 ⁷Department of Archaeology, University of Durham, Durham, United Kingdom.

23 ⁸Department of Forensic Medicine and Toxicology, School of Medicine, National and
24 Kapodistrian University of Athens, Athens 11527, Greece.

25 ⁹Department of Evolutionary Biology, University of Vienna, Vienna 1090, Austria.

26 ¹⁰Institute for Oriental and European Archaeology, Austrian Academy of Sciences,
27 Vienna 1020, Austria.

28

29 **Declaration of interest:** none

30

31 **Correspondence to:**

32 Fotios Alexandros Karakostis

33 Senckenberg Centre for Human Evolution and Palaeoenvironment,

34 University of Tübingen,

35 Rümelinstrasse 23, Tübingen 72070, Germany.

36 E-mail: fotios-alexandros.karakostis@uni-tuebingen.de

37

38

39

40 **Abstract**

41

42 Until the early 5th century BC, Phaleron Bay was the main port of ancient Athens
43 (Greece). On its shore, archaeologists have discovered one of the largest known
44 cemeteries in ancient Greece, including a range of burial forms, simple pits,

45 cremations, *larnaces* (clay tubs), and series of burials of male individuals who appear
46 to have died violent deaths, referred to here as “atypical burials”. Reconstructing the
47 osteobiographies of these individuals will help create a deeper understanding of the
48 socio-political conditions preceding the rise of Classical Athens. Here, we assess the
49 habitual manual behavior of the people of Archaic Phaleron (ca. 7th – 6th cent. BC),
50 relying on a new and precise three-dimensional method for reconstructing physical
51 activity based on hand muscle attachment sites. This approach has been recently
52 validated on laboratory animal samples as well as on recent human skeletons with a
53 detailed level of lifelong occupational documentation (i.e., the mid-19th century Basel
54 Spitalfriedhof sample). Our Phaleron sample consists of 48 adequately preserved hand
55 skeletons, of which 14 correspond to atypical burials. Our results identified consistent
56 differences in habitual manual behaviors between atypical burials and the rest. The
57 former present a distinctive power-grasping tendency in most skeletons, which was
58 significantly less represented in the latter (p-values of <0.01 and 0.03). Based on a
59 comparison with the uniquely documented Basel sample (45 individuals), this
60 enthesal pattern of the atypical burials was exclusively found in long-term heavy
61 manual laborers. These findings reveal an important activity difference between
62 burials typical for the Phaleron cemetery and atypical burials, suggesting that the
63 latter were likely involved in distinctive, strenuous manual activities. The results of
64 this pilot study comprise an important first step towards reconstructing the identity of
65 these human skeletal remains. Future research can further elucidate the occupational
66 profiles of these individuals through the discovery of additional well-preserved hand
67 skeletons and by extending our analyses to other anatomical regions.

68

69 **Keywords:** physical activity, hand muscle attachments, entheses, three-dimensional
70 multivariate analysis, Archaic Greece, V.E.R.A. method.

71

72 **1. Introduction**

73

74 Phaleron (Palaio Faliro) lies on a bay of the Saronic Gulf, situated about four
75 km southwest of the Acropolis of the city of Athens, Greece. During most of the
76 Archaic period (700 to 480 BCE), it served as the main port of the city-state of Athens
77 (Osborne, 2009), until it was displaced to Piraeus in the early 5th century BC (Camp,
78 2001; Edwards et al., 1970). Recent excavations in the port area, during the
79 construction of the Stavros Niarchos Foundation Cultural Center, produced over 1,000
80 burials, excavated between 2012-2017 (Ingvarsson-Sundström & Backstrom, 2019;
81 Prevedorou & Buikstra, 2019; Chryssoulaki, 2020). The remains excavated during
82 2012-2013 anchor this study. The presence of individuals in unusual burial postures,
83 some apparently restrained by shackles or cord bindings, intermixed with typical
84 burials along with a lack of grave embellishments and funerary monuments, has led to
85 emphasis upon the non-elite status of those interred in the Phaleron cemetery
86 (Ingvarsson-Sundström & Backstrom, 2019; Chryssoulaki, 2020). The lack of grave
87 accoutrements contrasts with the elaborations present at cemeteries, such as the
88 Kerameikos in Athens (Lagia, 2000).

89 To date, more than 1,700 skeletons have been excavated in Phaleron, arranged
90 either in mass or individual burials (Ingvarsson-Sundström and Backstrom, 2019;
91 Prevedorou and Buikstra, 2019). The majority of these involves simple pit graves,
92 followed by pot burials, cremations with funeral pyres, stone-lined cist graves,

93 larnakes as well as a few less usual cases (e.g., a few tile graves or a wooden boat
94 used as a coffin) (Ingvarsson-Sundström and Backstrom, 2019). Conspicuous among
95 this variety of burial features are a variety of “atypical” burials, so-called because they
96 present evidence for captivity and execution (e.g., shackled or otherwise restrained
97 individuals) and unusual burial treatments (e.g., prone or with feet & hands bound
98 together) (Ingvarsson-Sundström & Backstrom, 2019). These “atypical” burials,
99 recovered from pits, are those termed “biaiothanatoi” by Ingvarsson-Sundström &
100 Backstrom (2019) and by Chryssoulaki (2020), who attribute them to a violent death.
101 Similar burials, including apparent examples of crucified individuals, had been
102 excavated at Phaleron early in the 20th century (Keramopoulos, 1923; Pelekidis,
103 1916).

104 The “Phaleron Bioarchaeological Project” (PBP) of the Malcolm H. Wiener
105 Laboratory of the American School of Classical Studies at Athens (ASCSA) holds the
106 permit for conservation and study of the remains excavated during 2012 and 2013.
107 The PBP is constructing an osteobiography for each individual interred at the site,
108 then making comparisons across the site, grouping burial contexts by location and by
109 type. In this example, we will compare “typical” burials to those buried atypically
110 individually or in smaller groups. We focus here upon the occupational manual
111 activities of these individuals and groups.

112 In the absence of textual information, we must rely on skeletal information to
113 reconstruct activities related to occupational specialization. There are several
114 anthropological methods proposed for reconstructing habitual physical activity based
115 on human skeletal remains (Larsen, 1999; Pearson and Lieberman, 2004). One of the
116 most frequent avenues focuses on bony changes occurring in the areas where muscles
117 attach (i.e., “entheses”) (Foster et al., 2014; Henderson et al., 2017; Schrader, 2019)

118 Several approaches to analyzing entheses have been proposed, the majority of which
119 relies on detailed protocols for visual evaluation of enthesal robusticity and/or
120 potential enthesopathies (Henderson et al., 2017; Mariotti et al., 2007, 2004; Villotte,
121 2006; Villotte et al., 2010; Villotte and Knüsel, 2013), often providing crucial insights
122 into past human lifeways (e.g., Havelková et al., 2011; Villotte et al., 2010; Villotte
123 and Knüsel, 2014). Other analytical approaches have focused on the three-
124 dimensional (3D) form of entheses, relying on quantitative analyses of their 3D size
125 and/or shape (e.g., Karakostis et al., 2018a; 2017; Karakostis and Lorenzo, 2016;
126 Noldner and Edgar, 2013; Nolte and Wilczak, 2013; Williams-Hatala et al., 2016).
127 However, the overall reliability of most previous approaches using entheses to
128 reconstruct activity in the past have often been questioned (e.g., Foster et al. 2014). In
129 particular, previous studies have highlighted the low intra- and inter- observer
130 repeatability of most visual scoring systems that focus explicitly on enthesal
131 robusticity (Davis et al., 2013; Jorgensen et al., 2020; Wilczak et al., 2016), a reported
132 lack of association between entheses and cross-sectional morphology (which is widely
133 used for reconstructions of activity) (e.g., Michopoulou et al., 2017; Nikita et al.,
134 2019), an absence of association between the size of a muscle and enthesal raw
135 dimensions (Williams-Hatala et al., 2016; but see also the results of Bucchi et al.,
136 2019; Deymier-Black et al., 2015; Karakostis et al., 2019a), as well as a broader lack
137 of experimental validation (Wallace et al., 2017; Zumwalt, 2006).

138 To address these concerns, some of us have recently put forth a new and
139 repeatable approach for reconstructing activity using muscle attachment sites
140 (Karakostis & Harvati, 2021; Karakostis and Lorenzo, 2016), which is the first to be
141 validated based on two laboratory animal samples (Karakostis et al., 2019a, 2019b) as
142 well as on human skeletons with a unique level of life-long and detailed occupational

143 documentation (Karakostis et al., 2017). In contrast to previous methods, this
144 approach relies on a precise protocol for 3D quantification of enthesal surface areas,
145 followed by the identification of correlations among different entheses that reflect
146 standard muscle synergy groups (e.g., for power- or precision- grasping hand
147 movements) (Karakostis et al., 2017, 2019a; Karakostis & Lorenzo, 2016). To date,
148 except for our experimental studies on laboratory animal species, our research has
149 mainly focused on muscle attachment sites of the human hand, mainly due to its
150 fundamental role in most daily human activities (for biomechanical arguments, see
151 Karakostis et al., 2019c). Recently, the application of this novel approach on
152 paleoanthropological and bioarchaeological contexts has provided important insights
153 into the habitual manual behavior of Neanderthals as well as modern humans from
154 various geo-chronological contexts, establishing original and meaningful connections
155 between biological and cultural lines of evidence (e.g., Karakostis et al., 2020;
156 Karakostis, et al., 2018; Karakostis & Lorenzo, 2016). In a recently published review
157 (Karakostis & Harvati, 2021), this new approach has been named the “Tübingen
158 University Validated Entheses-based Reconstruction of Activity” (V.E.R.A.) method.

159 The aim of this study is to reconstruct patterns of manual physical activity of
160 the people of Phaleron, comparing those from “typical” burials to the atypical ones.
161 For this purpose, we apply the above described experimentally validated methodology
162 (i.e., the V.E.R.A. protocols) on two groups of well-preserved hand skeletons, (1) the
163 “typical burials” from across the cemetery, and (2) the “atypical burials”, which have
164 been defined as “biaiothanatoi” (Ingvarsson-Sundström & Backstrom, 2010;
165 Chryssoulaki, 2020). Furthermore, we compare the hand enthesal patterns of these
166 skeletons with those of a reference sample with uniquely detailed and lifelong
167 occupational documentation (i.e., the mid-19th century Basel Spitalfriedhof sample;

168 see Hotz & Steinke, 2012; Karakostis et al., 2017). Our resulting observations provide
169 new insights into the manual activity patterns of these individuals, setting the base for
170 further inter-disciplinary research.

171

172 **2. Materials and Methods**

173

174 **2.1 Sampling strategy**

175 In this pilot study, our sample of atypical burials consists of 14 adequately
176 preserved hand skeletons, including bone elements from both anatomical sides. Their
177 basic anthropological analysis indicated that they were all probable or possible males,
178 which will be considered “male” for the remainder of this report. This assessment
179 relies on the standards described in Buikstra & Ubelaker (1994). Particularly,
180 biological sex was estimated based on morphological traits of the pelvis and the skull.
181 Regarding the pelvis, we relied on the criteria proposed by Phenice (1969) and revised
182 by Klales et al. (2012), involving the visual evaluation of the ventral arc, subpubic
183 concavity, and ischio-pubic ramus. We additionally recorded the greater sciatic notch
184 of the ilium, following Walker (2005; after Buikstra and Ubelaker, 1994). Even
185 though estimations relying on the greater sciatic notch are less reliable than the ones
186 based on the pubic bones, the greater sciatic notch was more frequently preserved in
187 the Phaleron individuals. Sex determination based on the skull relied on the widely
188 used criteria proposed by Walker (2008; after Buikstra & Ubelaker, 1994). Overall,
189 when the pubic bone was available, its dimorphic markers were privileged due to their
190 verified accuracy (Klales et al., 2012).

191 Biological age was assessed based on morphological changes in the os coxa
192 (i.e., the pubic symphysis and the auricular surface), epiphyseal union (occurring in
193 early adulthood), and the degree of cranial suture closure. Degenerative changes at the
194 surface of the pubic symphysis were evaluated based on the Hartnett-Fulginiti
195 revision (Hartnett, 2010) of the Suchey-Brooks method (Brooks & Suchey, 1990),
196 whose improved accuracy and precision have been demonstrated (Merritt, 2015). In
197 this study, we estimated age based on multiple skeletal indicators, relying on a
198 transition analysis that involved the pubic symphysis, auricular surface, and cranial
199 sutures. This procedure led to the calculation of a maximum likelihood estimate and a
200 95% confidence interval of age for each individual (Milner & Boldsen, 2016). It
201 should be noted that, in cases of inconsistent estimates among indicators, or when a
202 single indicator provided a more precise age estimate, the pubic symphysis was
203 favored due to its demonstrated reliability (Merritt, 2015). For estimating the final age
204 of young adults, epiphyseal union was privileged, whereas cranial suture closure was
205 only used when the other indicators were not preserved. In the present study, the hand
206 bones of all individuals presented fused epiphyses. Due to preservation issues, a
207 relatively narrow age-range could be estimated only for six of the atypical burials,
208 including four young (less than ca 35 years old) and two relatively old (over ca 55
209 years of age) individuals. For the rest, an estimated age range could either not be
210 provided at all or it was too broad to be useful (see Materials and Methods). It should
211 be highlighted that future research would greatly benefit from the potential analysis of
212 additionally discovered well-preserved hand skeletons from the Phaleron cemetery
213 (for example, those excavated in later years; see Ingvarsson-Sundström & Backstrom,
214 2019; Chryssoulaki, 2020; Prevedorou & Buikstra, 2019;).

215 Our general, typical burial sample involves 34 individual skeletons, which
216 were discovered in 29 pit graves, four cist (or cist-like) graves, and a jar burial. This
217 sample was composed of 11 probable or possible females, 21 probable or possible
218 males, and two cases of undetermined sex. We will simply report these as “males’ and
219 “females” and “indeterminate” for the remainder of this research paper. A relatively
220 narrow age-range could be determined for 15 young (below ca 35 years old), six
221 relatively older (above ca 35 years old), and two late subadult (or possibly young
222 adult) individuals.

223 Our comparative analysis also includes a sample of 45 extensively
224 documented individuals from the historical Basel-Spitalfriedhof collection (Natural
225 History Museum in Basel, Switzerland), who lived in the broader region of the city of
226 Basel during the mid-19th century (Hotz and Steinke, 2012; Karakostis et al., 2017).
227 These were all adult males of low to middle socioeconomic status, between 18 and 48
228 years of age, whose hands presented no pathological conditions. Based on their
229 genealogical records, none of these individuals were directly related to one another
230 (Hotz & Steinke, 2012; Karakostis et al., 2017). Our past research has often relied on
231 this modern comparative sample due to its unique level of occupational
232 documentation for each person. In particular, the archives describe each individual’s
233 occupation, duration of each job, exact position at work, and hiring institution or
234 company. Moreover, there is information on the individuals’ genealogical relations,
235 official medical records, as well as socioeconomic characteristics (Hotz & Steinke,
236 2012; Karakostis et al., 2017). Based on this longitudinal documentation, 23 of the
237 sampled individuals were involved in heavy manual labor (i.e., mainly long-term
238 construction workers of different outdoor specialties), whereas the other 22 spent their
239 lives performing finer and/or semi-mechanized tasks (e.g., full-time tailors and

240 painters) (Karakostis et al., 2017). A previous application of our 3D multivariate
241 methodology on this reference sample identified clear differences between lifelong
242 heavy manual laborers (showing a distinctive power-grasping enthesal pattern) and
243 long-term precision workers of lower intensity (exhibiting a consistent precision-
244 grasping enthesal pattern involving a coordination between the thumb and index
245 finger muscles) (Karakostis et al., 2017). In more recent research, the thorough
246 documentation provided by this comparative sample helped our approach to interpret
247 the grasping differences observed in unidentified bioarchaeological samples,
248 including relatively recent case-studies (e.g., Hotz, 2017), a late medieval population
249 from Burgos (Karakostis & Lorenzo, 2016), as well as prehistoric hunter-gatherers
250 from diverse geo-chronological contexts (Karakostis et al., 2020, 2018b).

251 Following the results of our previous studies (Karakostis et al., 2020, 2018b,
252 2017; Karakostis and Lorenzo, 2016), we initially focused on nine hand muscle
253 attachment sites. However, given the underrepresentation of certain bone elements in
254 the Phaleron sample, our study relied on a total of five entheses, corresponding to six
255 thumb muscles with central importance in human hand biomechanics (Clarkson,
256 2000; Karakostis et al., 2017; Karakostis & Lorenzo, 2016; Marzke et al., 1998).
257 These involve the common attachment area of muscles *abductor pollicis brevis* and
258 *flexor pollicis brevis* (ABP/FPB) as well as the insertion sites of muscles *opponens*
259 *pollicis* (OP), *adductor pollicis brevis* (ADP), *extensor pollicis brevis* (EPB), and
260 *flexor pollicis longus* (FPL). The general characteristics of these muscles and entheses
261 (including the bones on which they are located) are summarized in Table 1. It is worth
262 noting that these enthesal surfaces did not seem to present distinguishable
263 pathological alterations in the individuals of our sample.

264

| Muscles | Abbreviation | Main action | Analyzed attachment site |
|---------------------------------|---------------------|--|--|
| <i>Abductor pollicis</i> | ABP | Abducts the thumb | Radial base of the first proximal phalanx |
| <i>Flexor pollicis brevis</i> | FPB | Flexes the first metacarpophalangeal joint | (same enthesal area for both muscles) |
| <i>Adductor pollicis</i> | ADP | Adducts the thumb | Ulnar base of the first proximal phalanx |
| <i>Extensor pollicis brevis</i> | EPB | Extends the thumb | Dorsal base of the first proximal phalanx |
| <i>Opponens pollicis</i> | OP | Abducts, rotates, and flexes the thumb | Radial diaphysis of the first metacarpal |
| <i>Flexor pollicis longus</i> | FPL | Flexes the first distal phalanx | Palmar diaphysis of the first distal phalanx |

265

266 **Table 1. The anatomical location of the five muscle attachment sites used, their**
267 **abbreviation, and the function of their six associated muscles.**

268

269 **2.2 Precise 3D measurement of muscle attachment sites**

270 The 3D surface of all hand bones was reconstructed using a handheld Artec
271 Space Spider scanner (Artec Inc., Luxembourg). This equipment relies on structured-
272 light technology, providing scans with a measuring accuracy of 50 microns. The
273 developed 3D models were exported in PLY format and imported into the software
274 Meshlab (Meshlab Inc., Rome) for further surface processing and analysis.

275 For delineating the exact borders of entheses on the bone surface, we
276 employed the detailed protocols of the V.E.R.A. approach, whose intra- and inter-
277 observer repeatability has been verified in previous research on the same hand muscle
278 attachment sites (maximum mean error was 0.62%; see Karakostis & Lorenzo, 2016).
279 In more recent work, the exact steps of this protocol were described in greater detail,
280 including illustrations of all steps in Karakostis & Harvati (2021) (for experimental
281 animal studies, also see Karakostis et al., 2019). In brief, enthesal borders are

282 virtually defined on the bone meshes based on the criteria of surface elevation,
283 irregularity, and coloration. The most defining criterion is surface elevation (i.e., the
284 presence of projecting or depressing bone area). This process is greatly facilitated by
285 various 3D imaging filters, which are available in the open-access software Meshlab.
286 Initially, the broader enthesal area is identified on the bone using standard surface
287 curvature algorithms (such as the filter “Discrete curvatures”). Then, the observer
288 selects a region of the bone that encompasses both the distinctive attachment site as
289 well as a thin zone of relatively flatter surface around the attachment site.
290 Subsequently, applying additional filters exclusively on that bone region (i.e.,
291 “Curvature principal directions”, “Distance from borders”, or “Calculation of
292 geodesic distances”) helps identifying the exact borders of entheses on the bone
293 surface and allows for a direct quantification of their 3D surface areas (in mm²).

294

295 **2.3 Statistical analyses**

296 Following the V.E.R.A. protocols, the calculated 3D surface areas of all five
297 entheses (in mm²) were used as variables in a series of principal component analyses
298 (PCAs). These relied on a correlation matrix because the variables presented varying
299 scales (Table 2). For all PCAs, the variables of our dataset met the assumptions for a
300 PCA (Field, 2013), including minimum sample size requirements (i.e., a minimum of
301 five cases per variable), approximately normal distribution (based on normal
302 probability plots), sphericity (based on Bartlett’s tests), linearity among variables
303 (based on bivariate plots), and no outliers (according to the z-scores technique). The
304 number of the principal components (PCs) plotted for each PCA was decided based
305 on the standard scree-plot approach (Cattell, 1966; Field, 2013). All statistical

306 analyses of this study were carried out in the software IBM SPSS (IBM inc., Armonk,
 307 NY; version 24 for Windows). No PCA conducted in this study assumed prior group
 308 assumptions for the individuals (i.e., in the plots, cases were simply colored by group
 309 after the analysis).

310

| Anatomical side | Muscle attachment site | Atypical burials | | Typical burials | |
|-----------------|------------------------|------------------|-------------------|-----------------|-------------------|
| | | N | Mean \pm SD | N | Mean \pm SD |
| Combined sides | ABP / FPB | 14 | 76.88 \pm 26.72 | 35 | 62.98 \pm 16.83 |
| | ADP | 14 | 58.33 \pm 18.48 | 35 | 50.05 \pm 14.31 |
| | EPB | 14 | 66.74 \pm 22.16 | 34 | 43.28 \pm 17.06 |
| | OP | 11 | 90.09 \pm 24.76 | 33 | 78.61 \pm 19.24 |
| | FPL | 11 | 38.29 \pm 8.78 | 22 | 30.06 \pm 10.97 |
| Right | ABP / FPB | 11 | 81.06 \pm 23.40 | 27 | 60.86 \pm 16.28 |
| | ADP | 11 | 60.18 \pm 18.65 | 26 | 49.47 \pm 13.85 |
| | EPB | 10 | 68.87 \pm 26.17 | 24 | 42.49 \pm 15.33 |
| | OP | 12 | 83.15 \pm 28.04 | 27 | 77.61 \pm 19.93 |
| | FPL | 8 | 38.87 \pm 7.63 | 20 | 31.24 \pm 11.39 |
| Left | ABP / FPB | 9 | 73.69 \pm 21.87 | 31 | 59.52 \pm 15.49 |
| | ADP | 9 | 61.54 \pm 17.12 | 32 | 50.39 \pm 13.21 |
| | EPB | 8 | 65.94 \pm 14.16 | 28 | 41.18 \pm 18.21 |
| | OP | 6 | 71.69 \pm 23.36 | 30 | 70.71 \pm 19.54 |
| | FPL | 8 | 34.18 \pm 8.15 | 14 | 27.61 \pm 8.83 |

311

312 **Table 2. Descriptive statistics for each variable (i.e., 3D surface area**

313 **measurements for each enthesis, in mm²) per Phaleron burial group and**

314 **anatomical side, including sample size (N), mean, and standard deviation (SD).**

315 Muscle abbreviations are provided in Table 1. Each variable's sample size (N) does

316 not correspond to the number of individuals used in the PCAs (Figs. 1 to 7; Table 3),

317 which require the use of individual hand skeletons with all necessary entheses

318 preserved (i.e., all first three entheses for the first PCA and all five entheses for the
 319 second PCA).

320

321 A separate analysis was conducted for each anatomical side. The resulting
 322 multivariate patterns were generally symmetrical (see Table 3 and figures in Results).
 323 It should be noted, however, that the PCA based on five entheses (see below) could
 324 not be performed for the left anatomical side since only one atypical burial presented
 325 all five left muscle attachment sites. To maximize sample representation, we
 326 additionally performed a mixed sides analysis that combined an individual's left and
 327 right entheses. The best-preserved side (left or right) was defined based on the number
 328 of healthy entheses present. When an enthesis was missing from that side, this was
 329 taken from the less-preserved side, allowing the specimen to participate in the PCA.
 330 In the few cases of perfectly equal preservation between the two sides, the right side
 331 was preferred since the right entheses were overall much better preserved both in the
 332 Phaleron as well as the Basel samples. Considering that the observed patterns among
 333 groups were highly consistent between the combined sides PCA analyses (Figs. 1 to
 334 4; Table 3) and those relying on each side separately (Figs. 2, 3 and 5 to 7; also see
 335 PCA statistics in Table 3), our subsequent statistical comparisons focused on the
 336 combined PCAs.

337

338

| Analyses | Eigenvalue | Variance explained (%) | Factor loadings | | | | |
|-----------------------|------------|------------------------|-----------------|-------|------|----|-----|
| | | | ABP/FPB | ADP | EPB | OP | FPL |
| Combined sides | | | | | | | |
| First PCA | | | | | | | |
| PC1 | 2.03 | 67.66 | 0.90 | 0.85 | 0.71 | | |
| PC2 | 0.68 | 22.61 | -0.19 | -0.39 | 0.70 | | |

| | | | | | | | | |
|-----------------------|--------------|------|-------|-------|-------|-------|------|-------|
| | Total | | 90.28 | | | | | |
| Combined sides | | | | | | | | |
| Second PCA | | | | | | | | |
| | PC1 | 2.71 | 54.18 | 0.92 | 0.82 | 0.63 | 0.45 | 0.77 |
| | PC2 | 0.99 | 19.83 | 0.13 | -0.11 | -0.16 | 0.87 | -0.42 |
| | PC3 | 0.70 | 14.02 | -0.14 | -0.29 | 0.75 | 0.04 | -0.17 |
| | Total | | 88.03 | | | | | |
| Right side | | | | | | | | |
| First PCA | | | | | | | | |
| | PC1 | 1.94 | 64.66 | 0.86 | 0.81 | 0.74 | | |
| | PC2 | 0.65 | 21.69 | -0.14 | -0.45 | 0.65 | | |
| | Total | | 86.35 | | | | | |
| Right side | | | | | | | | |
| Second PCA | | | | | | | | |
| | PC1 | 2.61 | 52.17 | 0.87 | 0.75 | 0.65 | 0.47 | 0.81 |
| | PC2 | 0.97 | 19.42 | 0.19 | -0.25 | -0.17 | 0.86 | -0.33 |
| | PC3 | 0.71 | 14.24 | -0.14 | -0.41 | 0.72 | 0.03 | -0.07 |
| | Total | | 85.82 | | | | | |
| Left side | | | | | | | | |
| First PCA | | | | | | | | |
| | PC1 | 1.98 | 65.92 | 0.86 | 0.86 | 0.71 | | |
| | PC2 | 0.67 | 22.29 | -0.29 | -0.29 | 0.71 | | |
| | Total | | 88.21 | | | | | |

339

340 **Table 3. Statistics of the principal component analyses performed, either on**
341 **three (first PCA) or five muscle attachment sites (second PCA). Muscle**
342 **abbreviations are provided in Table 1.**

343

344 Furthermore, following previous applications of our approach (Karakostis et
345 al., 2018b), two different PCAs were run for each side separately as well as the
346 combined dataset. The first PCA attempted to further maximize the sample size of our
347 analysis by relying on three entheses that correspond to four thumb muscles that play
348 a central role in hand biomechanics. These entheses correspond to four muscles

349 inserting into the 1st proximal phalanx (Table 1): ABP/FPB, ADP, and EPB. Our
350 previous research on these three muscle attachment sites showed that they could
351 provide a considerable separation between lifelong occupational tendencies
352 (Karakostis et al., 2018b). The second PCA attempted to maximize the number of
353 enthesal variables, relying on all five muscle attachment sites, thus also considering
354 the important contribution of muscles OP and FPL (Table 1). Both PCAs identified a
355 principal axis of variation explaining differences between power- and precision-
356 grasping enthesal patterns (e.g., see Karakostis et al., 2017, 2018).

357 We further evaluated the observed differences between atypical and typical
358 burials using the two-sample Kolmogorov-Smirnov Z test (Corder and Foreman,
359 2014), a non-parametric analysis that has been recommended for comparing groups
360 with small sample sizes (Field, 2013). We focused on the scores of selective PCs that
361 exhibited distinctive variation between the two burial groups (see Results and
362 figures). Furthermore, for the scores of PC2 (from the second PCA) that presented
363 inter-population variation, we also tested for significant differences between all
364 Phaleron and all Basel individuals. In order to control for the probability of increased
365 Type 1 error (due to the three comparisons performed), we confirmed that p-values
366 were still significant after adjusting them based on the Holm-Bonferroni sequential
367 technique (Holm, 1979). Additionally, the same comparisons were applied for the raw
368 3D surface size (in mm²) of each of the five entheses analyzed in this study.

369 Finally, to account for the potential effects of biological age and body size on
370 the observed multivariate patterns (PC scores), we assessed the strength of their
371 association with biological age and estimated stature using the Spearman's correlation
372 coefficient (r_s). Given that an exact age-group (i.e., young, middle aged, or old) and
373 approximate stature could not be reliably indicated for most of our sample's 14

374 atypical burials, these statistical tests were applied only on the values of our
375 documented reference sample from Basel (see in Karakostis et al., 2017).
376 Nevertheless, we also provide general remarks regarding the potential effects of age
377 on the PCA results for the Phaleron samples (see Results), focusing on the individuals
378 for which an approximate estimation of age-group was available.

379

380 **3. Results**

381

382 The basic characteristics of this study's variables are provided for each
383 anatomical side in Table 2. All PCA statistics (eigenvalues, percentages of variance,
384 and factor loadings) are presented in Table 3. As it can be observed in Table 3 and the
385 figures (Figs. 1 to 7), all the statistics and multivariate patterns described below were
386 consistently similar between the combined-sides PCAs and the PCAs on each side
387 separately (also see Discussion).

388 For the combined-sides first PCA, which was based on three enthesal
389 variables, the scree-plot approach recommended focusing on PC1 and PC2,
390 representing a total of 90.2% of total variance in the sample (Fig. 1). Based on the
391 factor loadings (Table 3), PC1 (67.4% of the sample's variance) represented overall
392 size differences across specimens (i.e., all factor loadings were positive), indicating
393 that individuals with higher PC1 scores presented overall larger entheses. In contrast,
394 variation on PC2 (22.8%) reflects the proportion between two entheses of three thumb
395 thenar muscles (ABP_FPB and ADP) and the insertion site of EPB, a thumb's main
396 extensor muscle (Table 1). Both Phaleron groups extensively overlap on PC1, despite
397 a clear tendency of smaller enthesal size in the typical burial group (i.e., most cases

398 show low PC scores). On PC2, our documented sample's lifelong heavy manual
399 workers present distinctively higher positive scores (i.e., proportionally larger EPB),
400 whereas long-term precision workers show lower scores (i.e., proportionally larger
401 thenar muscles associated with flexion, abduction, and adduction at the trapezio-
402 metacarpal joint). This broadly reflects the results of our previous research for the
403 documented Basel sample (Karakostis et al., 2020, 2018b, 2017). On this axis, 11 of
404 the 14 atypical burials present distinctively higher scores, exclusively overlapping
405 with lifelong heavy manual laborers, while three of them show low scores and
406 coincide with long-term precision workers. Regarding the typical burial sample, even
407 though its majority overlaps with heavy manual laborers, their PC2 values are
408 consistently lower than those of the atypical burials. Moreover, several of their scores
409 (12/34) coincide with those of long-term precision workers. It is worth noting that the
410 males and females of this group exhibit similar PC2 values, but none of the 11
411 females show very high positive PC2 values (Fig. 1). Consequently, there is a distinct
412 area in the uppermost part of the PC2 axis that includes only males, including several
413 long-term heavy construction workers, most of the atypical burial sample (10 of 14),
414 and three individuals from the typical burial sample.

415

416

417

418

419

420

421

422

423

424

425

426

427

428

429

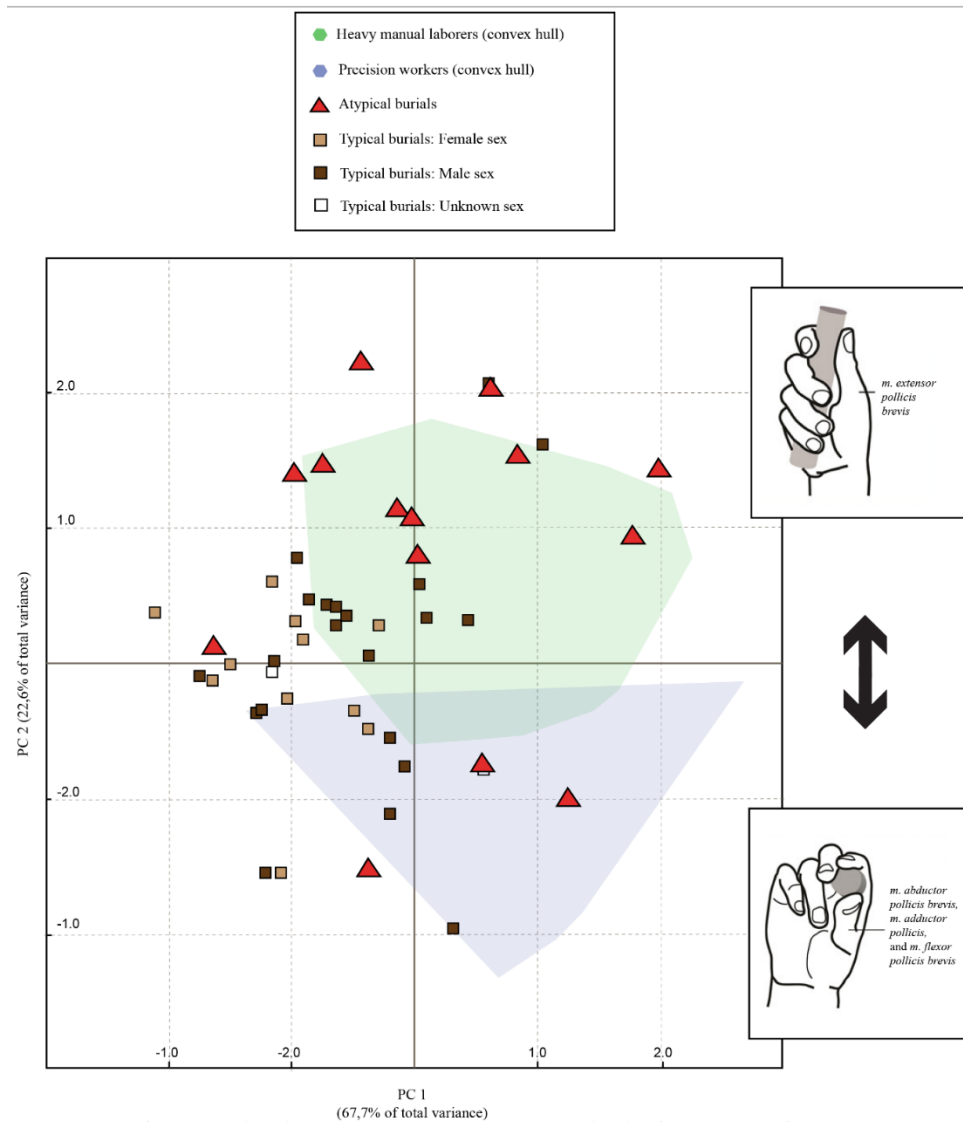
430

431

432

433

434



435

Figure 1. Plot of the principal component analysis (PC1 and PC2) based on the

436

3D area measurements of three muscle attachment sites and all individuals

437

preserving these entheses. This PCA was conducted on a dataset combining entheses

438

from both anatomical sides, after confirming that results were consistent across PCAs

439

(see Materials and Methods). No groups were assumed *a priori*. For the purpose of

440

visual clarity, the documented samples from Basel are only represented in the plot by

441

their convex hulls (for an extensive description of manual enthesal patterns in the

442 same exact individuals, see Karakostis et al., 2020, 2018, 2017). The upper side
443 illustration summarizes the main pattern presented by individuals with higher PC2
444 values (i.e., a proportionally larger entheses for *extensor pollicis brevis*; see Table 3),
445 while the lower side image is associated with cases with lower PC2 scores (i.e.,
446 proportionally larger attachment sites for muscles *abductor pollicis brevis*, *flexor*
447 *pollicis brevis*, and *adductor pollicis*; see Table 3). The two side figures were
448 modified after Karakostis et al. (2018).

449

450 For the combined second PCA (based on five entheses and fewer Phaleron
451 individuals), the scree-plot recommended focusing on the first 3 PCs (representing a
452 total of 88.0% of sample variance). As in the combined first PCA (Fig. 1), PC1
453 (54.2%) represents overall 3D size variation in the sample (Table 3; Figs 2 and 3),
454 while the factor loadings of PC3 (14.0%) are very similar to those of PC2 of the
455 combined first PCA (the one based on three entheses). Consequently, the observed
456 PC3 patterns are clearly equivalent, with 7 out of 9 atypical burials overlapping with
457 heavy manual laborers and two males from the general burial sample (Fig. 4).
458 Nevertheless, PC2 (19.8%) reveals a different pattern of variation in the sample. On
459 this axis, the two Phaleron samples broadly overlap in the positive side of the
460 component, while most Basel individuals present negative PC2 scores (see horizontal
461 PC2 axis of Fig. 4). Based on this PC2's factor loadings (Table 3), Phaleron
462 individuals consistently present a proportionally larger insertion site for OP, a muscle
463 of central importance for thumb opposition (Table 1). On this component, there is no
464 clear distinction between long-term heavy manual laborers and precision workers.

465

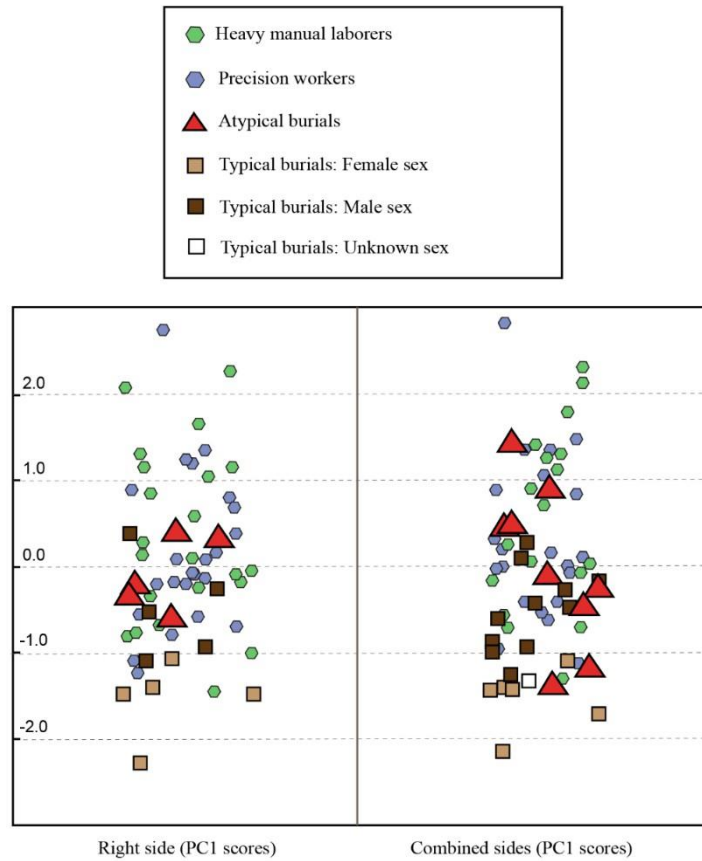
466

467

468

469

470



471

472

473

474

475

476

477 **Figure 2. Jitter plots presenting the principal component 1 (PC1) scores of the**
478 **two principal component analyses based on five muscle attachment sites (i.e., the**
479 **one on combined anatomical sides and the one only on the right hand entheses).**
480 **Based on the factor loadings (Table 3), interindividual variation on each of these**
481 **components represents differences in overall enthesal size (i.e., higher scores**
482 **represent larger sets of muscle attachment areas).**

483

484

485

486

487

488

489

490

491

492

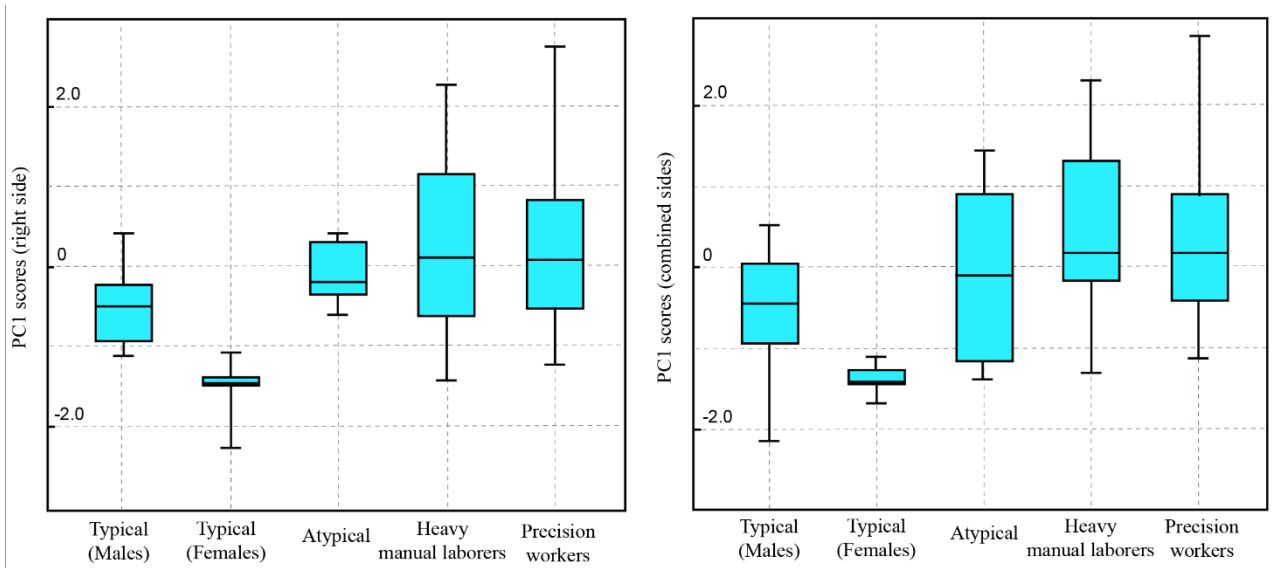
493

494

495

496

497



498

Figure 3. Boxplots presenting the principal component 1 (PC1) scores of the two

499

principal component analyses based on five muscle attachment sites (i.e., the one

500

on combined anatomical sides and the one only on the right hand entheses). Based on

501

the factor loadings (Table 3), interindividual variation on each of these components

502

represents differences in overall enthesal size (i.e., higher scores represent larger sets

503

of muscle attachment areas).

504

505

506

507

508

509

510

511

512

513

514

515

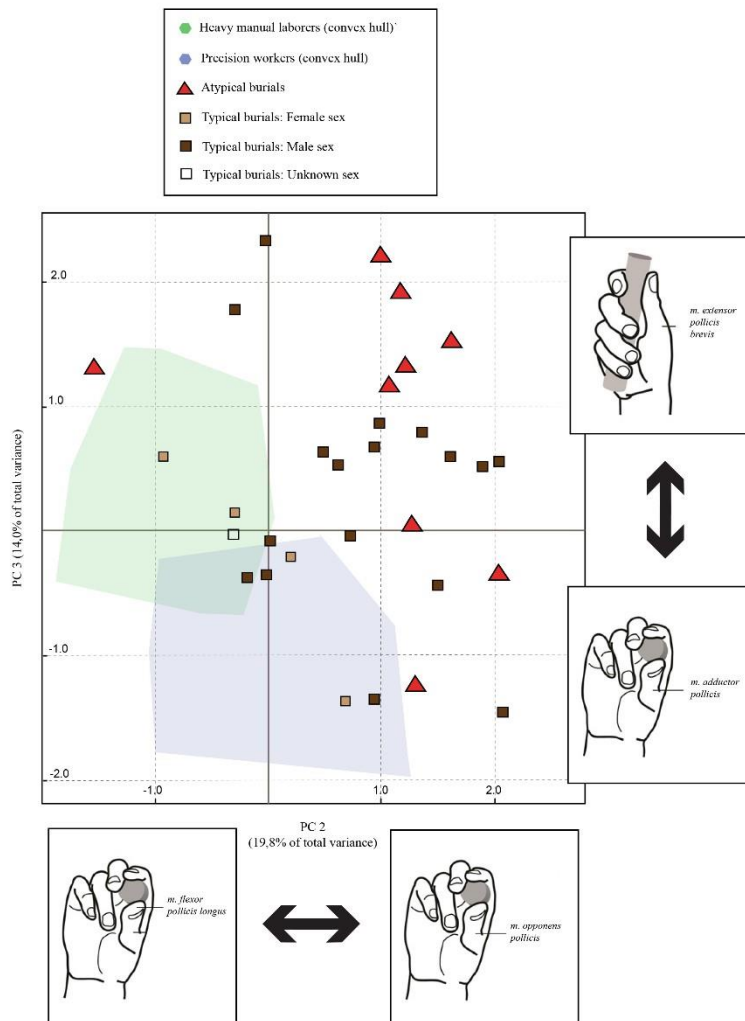
516

517

518

519

520



521 **Figure 4. Plot of the principal component analysis (PC2 and PC3) based on the**
522 **3D area measurements of five muscle attachment sites and all individuals**
523 **preserving these entheses.** This PCA was conducted on a dataset combining entheses
524 from both anatomical sides, after confirming that results were consistent across PCAs
525 (see Materials and Methods). No groups were assumed *a priori*. For the purpose of
526 visual clarity, the documented samples from Basel are only represented in the plot by
527 their convex hulls (for an extensive description of manual enthesal patterns in the
528 same exact individuals, see Karakostis et al., 2020, 2018, 2017). Reflecting the
529 vertical axis of the previous PCA (Fig. 1), the top illustration summarizes the main

530 pattern presented by individuals with higher PC3 scores, while the bottom image is
531 associated with cases with lower PC3 scores. Respectively, the side illustrations
532 summarize the main enthesal patterns of individuals with lower (left) and higher
533 (right) PC2 values (see Table 3). Variation on PC2 represents the proportional
534 enthesal size of muscle *opponens pollicis*. The four side figures were modified after
535 Karakostis et al. (2018).

536

537 As outlined in Materials and Methods, the main enthesal patterns observed
538 for the combined-sides dataset were also consistently present in the analyses focusing
539 on each anatomical side separately (see factor loadings for all PCAs in Table 3). The
540 latter include the two PCAs involving entheses of the right hand (Figs. 5 and 6; also
541 see PC1 scores in Figs. 2 and 3) as well as the PCA on three left enthesal
542 measurements (Fig. 7).

543

544

545

546

547

548

549

550

551

552

553

554

555

556

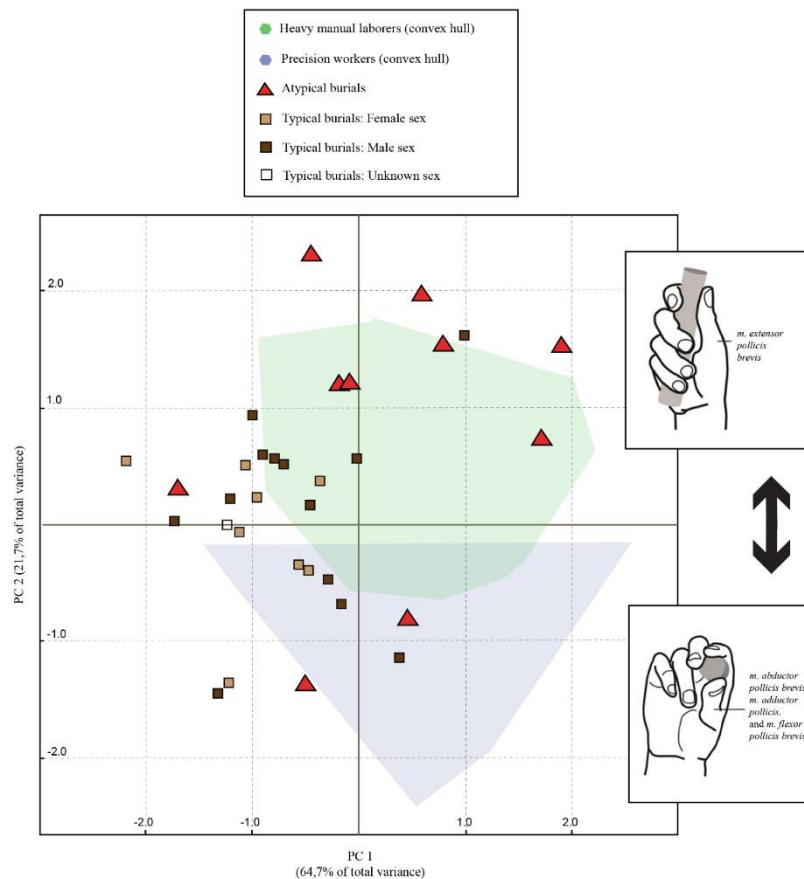
557

558

559

560

561



562

Figure 5. Plot of the principal component analysis (PC1 and PC2) based on the

563

3D area measurements of three right muscle attachment sites and all individuals

564

preserving these entheses. No groups were assumed *a priori*. For the purpose of

565

visual clarity, the documented samples from Basel are only represented in the plot by

566

their convex hulls (for an extensive description of manual enthesal patterns in the

567

same exact individuals, see Karakostis et al., 2020, 2018, 2017). Reflecting the

568

vertical axes of the PCAs on combined sides (Figs. 1 and 4), the top illustration

569

summarizes the main pattern presented by individuals with higher PC2 scores, while

570

the bottom image is associated with cases with lower PC2 values (see Table 3). The

571

two side figures were modified after Karakostis et al. (2018).

572

573

574

575

576

577

578

579

580

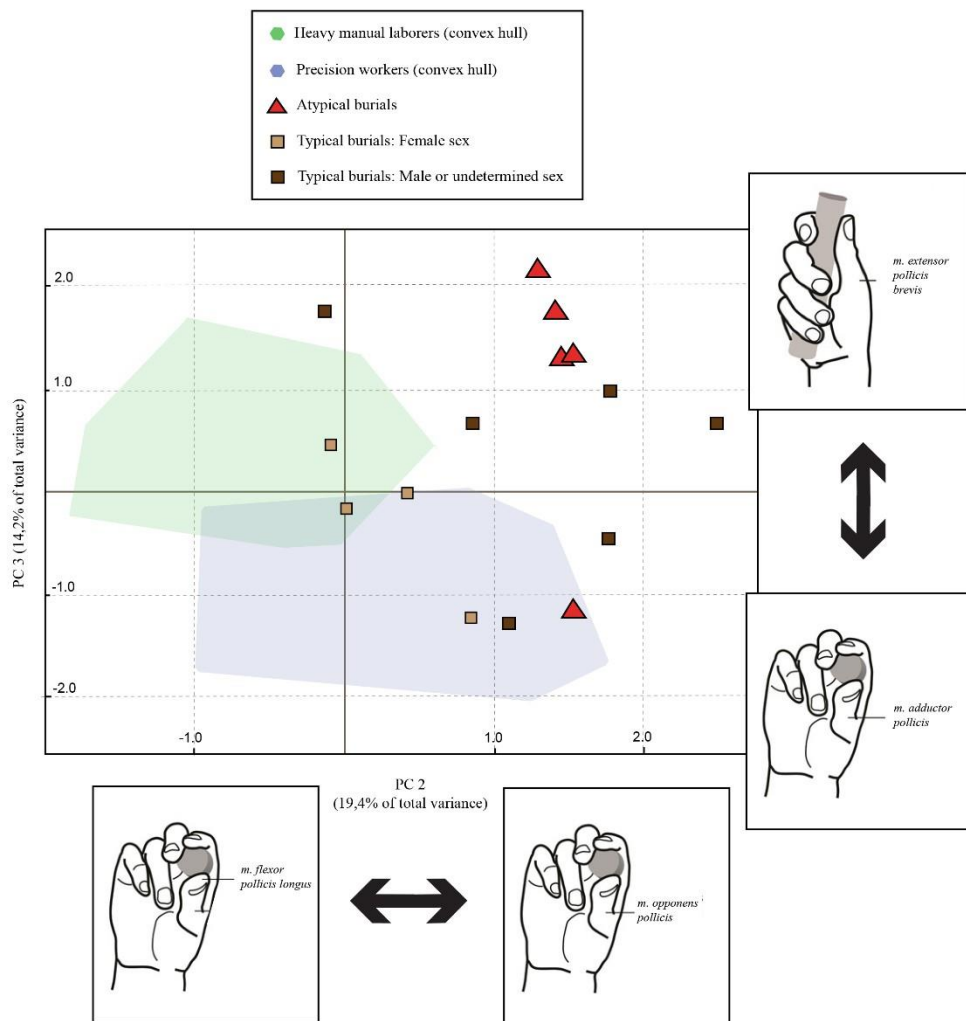
581

582

583

584

585



586 **Figure 6. Plot of the principal component analysis (PC2 and PC3) based on the**

587 **3D area measurements of five right muscle attachment sites and all individuals**

588 **preserving these entheses.** No groups were assumed *a priori*. For the purpose of

589 visual clarity, the documented samples from Basel are only represented in the plot by

590 their convex hulls (for an extensive description of manual enthesal patterns in the

591 same exact individuals, see Karakostis et al., 2020, 2018, 2017). Reflecting the

592 horizontal and vertical axes of the corresponding PCA on combined sides (Fig. 4), the

593 two top and two side illustrations summarize the main enthesal patterns observed in

594 each direction of the two components (see Table 3). The four side figures were

595 modified after Karakostis et al. (2018).

596

597

598

599

600

601

602

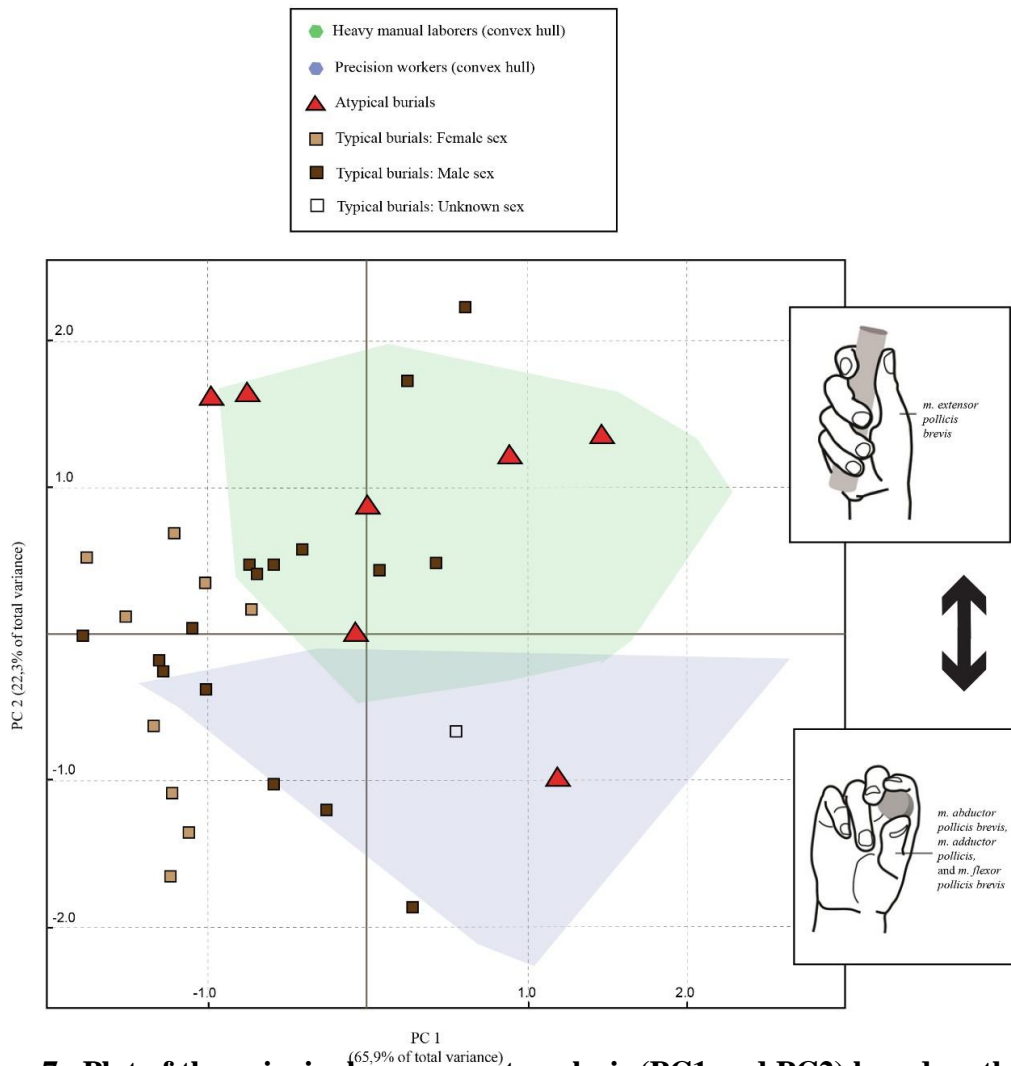
603

604

605

606

607



608

Figure 7. Plot of the principal component analysis (PC1 and PC2) based on the

609

3D area measurements of three left muscle attachment sites and all individuals

610

preserving these entheses. No groups were assumed *a priori*. For the purpose of

611

visual clarity, the documented samples from Basel are only represented in the plot by

612

their convex hulls (for an extensive description of manual enthesal patterns in the

613

same exact individuals, see Karakostis et al., 2020, 2018, 2017). Reflecting the

614

vertical axes of the PCAs on combined sides (Figs. 1 and 4) as well as the ones on

615

right hand entheses (Figs. 5 and 6), the top illustration summarizes the main pattern

616

presented by individuals with higher PC2 scores, while the bottom image is associated

617 with cases with lower PC2 values (see Table 3). The two side figures were modified
618 after Karakostis et al. (2018).

619

620 The results of the two-sample Kolmogorov-Smirnov Z tests further supported
621 the above observations of enthesal differences between burial groups (Table 4). A
622 statistically significant difference was found between typical and atypical burials in
623 the scores of both PC2 (in the first PCA; Fig. 1) and PC3 (in the second PCA; Fig. 4).
624 Furthermore, a significant difference was also found between all Phaleron and all
625 Basel individuals in the PC2 values of the second PCA (Fig. 4). In raw 3D size, EPB
626 showed a significant difference between burial groups, while four of the five entheses
627 significantly varied between Basel and Phaleron (Table 5).

628

| Groups compared | | Variable | Z-value | P-value |
|-----------------|------------------|-------------------------|---------|---------|
| Atypical | Typical | PC2 scores (first PCA) | 2.06 | < 0.01 |
| Atypical | Typical | PC3 scores (second PCA) | 1.46 | 0.03 |
| Phaleron | Reference sample | PC2 scores (second PCA) | 2.87 | < 0.01 |

629

630 **Table 4. Comparisons of multivariate patterns (PC scores) between groups using**
631 **the two-sample Kolmogorov-Smirnov Z tests.** All three p-values remained
632 statistically significant (below 0.05) even after correction using the Holm-Bonferroni
633 sequential technique (see Materials and Methods). The terms “atypical” and “typical”
634 refer to the two Phaleron burial groups studied, while “reference sample” indicates the

635 thoroughly documented individuals from the Basel Spitalfriedhof collection
 636 (Switzerland).

637

| Groups compared | | Raw Measurement | Z-value | P-value |
|-----------------|------------------|-----------------|---------|-----------------|
| Atypical | Typical | OP | 1.48 | 0.03 |
| Atypical | Typical | ABP/FPB | 1.22 | 0.10 |
| Atypical | Typical | ADP | 0.72 | 0.67 |
| Atypical | Typical | FPL | 1.35 | 0.05 |
| Atypical | Typical | EPB | 2.24 | <0.01 |
| Phaleron | Reference sample | OP | 1.63 | 0.01 |
| Phaleron | Reference sample | ABP/FPB | 1.60 | 0.01 |
| Phaleron | Reference sample | ADP | 2.31 | <0.01 |
| Phaleron | Reference sample | FPL | 4.00 | <0.01 |
| Phaleron | Reference sample | EPB | 1.07 | 0.20 |

638

639 **Table 5. Comparisons of raw 3D surface measurements (in mm²) between groups**
 640 **using the two-sample Kolmogorov-Smirnov Z tests.** P-values that remained
 641 significant after sequential correction (for each set of five comparisons; Field, 2013;
 642 Holm, 1979) are in bold. The terms “atypical” and “typical” refer to the two Phaleron
 643 burial groups studied, while “reference sample” indicates the thoroughly documented
 644 individuals from the Basel Spitalfriedhof collection (Switzerland). Abbreviations of
 645 muscle/entheses are spelled out in Table 1.

646

647 The results of the correlation tests on our documented reference sample
648 confirmed that the multivariate patterns observed in the PCAs (Figs. 1 and 4) were not
649 significantly associated with interindividual variation in biological age or stature.
650 Biological age and predicted stature were not correlated with the PCs that represented
651 variation in proportions among different entheses (i.e., PC2 of the first PCA, PC2 of
652 the second PCA, and PC3 of the second PCA), with p-values ranging between 0.12
653 and 0.74. In contrast, in agreement with previous studies (Karakostis et al., 2017;
654 Karakostis & Lorenzo, 2016), the components representing overall size variation (i.e.,
655 PC1 in both PCAs) were significantly and positively correlated with biological age (p-
656 value: 0.01; r_s : 0.46 and 0.47, respectively) and predicted stature (p-value < 0.01; r_s :
657 0.55, in both cases). This indicates a positive association between the raw size of
658 entheses and the individuals' age and estimated stature, suggesting that the observed
659 significant differences in raw 3D size (see comparisons listed in Table 5) may likely
660 be affected by systemic factors of interindividual enthesal variation (as also
661 demonstrated in previous studies; see extensive review by Karakostis & Harvati,
662 2021). Among the Phaleron individuals of our sample whose exact age-group could
663 be assessed (see Materials and Methods), there was no clear distinction across age-
664 groups within each sample. All calculated PCs for older and younger individuals
665 appeared to broadly overlap within each burial group. Nevertheless, it should be noted
666 that, for the atypical burial group, the two potentially older individuals (i.e., burials
667 IV_560 and 5_198) exhibited positive PC1 scores (i.e., larger overall enthesal 3D
668 size).

669

670

4. Discussion

671

672

673 The results of this study revealed a consistent power-grasping tendency in
674 most hand skeletons of the atypical burial sample (“biaiothanatoi”; Ingvarsson-
675 Sundström & Backstrom, 2019; Chryssoulaki, 2020), which led them to overlap
676 exclusively with documented long-term heavy manual laborers (Figs. 1 and 4 to 7;
677 also see Table 4). This tendency was present but distinctively lower in the individuals
678 of the general burial sample, several of which exhibited precision-grasping enthesal
679 patterns (overlapping with recent long-term precision workers). In terms of habitual
680 manual behavior, these results suggest that most individuals of our atypical burial
681 sample were involved in comparatively more strenuous activities than those in the
682 general burial sample. In our recent documented sample, similar enthesal patterns
683 were only found in long-term heavy manual laborers (mainly recent heavy
684 construction workers, such as bricklayers, carpenters, stonemasons, etc.). However, it
685 is crucial to clarify that this observed similarity does not indicate that the individuals
686 of the atypical burial sample themselves were necessarily construction workers, but
687 rather that their lifestyles likely shared a comparatively high frequency (and/or
688 intensity) of generalized power-grasping motions. Multiple strenuous manual
689 activities have been reported for the inhabitants of Archaic and Classical Athens, such
690 as farming, quarrying, mining, sea-faring, construction building, warfare, sports, and
691 others (Hall, 2007; Morris, 2009; Osborne, 2009). With the exception of warfare and
692 sports, most of these tasks were typically associated with individuals of lower or
693 middle socioeconomic status (Golden, 2009; Nicholson, 2011; Osborne, 2009;
694 Pritchard, 2012).

695 It is worth noting that all individuals of our atypical burial sample seem to be
696 of male sex (see Materials and Methods; also see Ingvarsson-Sundström &
697 Backstrom, 2019). In all our PCAs (Figs. 1 and 4 to 7), most of them occupied the
698 uppermost area of the plots (i.e., high scores on the vertical axes), overlapping
699 exclusively with certain male individuals of the typical burial group. This could
700 perhaps be indicative of behavioral differences between sexes, suggesting that some
701 of the males (including most atypical burials) may have been involved in more
702 strenuous manual tasks than all other males and females. However, given the limited
703 representation of potential female skeletons in our study (N=11), we believe that this
704 possibility can only be properly addressed through future research on increased
705 female sample sizes (in the atypical group). Additionally, considering the sexual
706 division of labor in Archaic Athens (Hall, 2007), one could argue that incorporating
707 females to analyses of male-only samples (i.e., atypical burials and the Basel
708 individuals) may have affected our results on manual activity. To ensure that this is
709 not the case, we have re-run all analyses without the 11 females, confirming that all
710 observed enthesal patterns (PCAs) as well as statistical test outputs (i.e., significance
711 of two-sample Kolmogorov-Smirnov results) did not considerably alter in any way.

712 Due to preservation issues, it was impossible to directly assess the effects of
713 biological age on the enthesal patterns of the Phaleron individuals. Nevertheless, our
714 tests focusing on the comparative sample from Basel showed that only PC1, which
715 reflected overall enthesal size (see factor loadings in Table 3), presented a strong
716 association with age and stature. On the contrary, the other PCs (PC2 and PC3),
717 which represented variation in proportions among different entheses, did not present
718 such correlations in the documented individuals. This directly reflects the results of
719 our previous research on the same mid-19th century Basel sample (Karakostis et al.,

720 2017). In the present study, on the PC1 axis, individuals from all groups (Basel and
721 Phaleron) extensively overlap in all analyses (e.g., see the PCA plot of Fig. 1). At the
722 same time, numerous individuals with almost identical values on PC1 (representing
723 overall size) present distinctive scores on the vertical axis PC2 (representing
724 proportions among different entheses), which is the variable demonstrating the group
725 differences highlighted in this study. Thus, if one were to propose a major effect of
726 biological age on the observed differences between typical and atypical burials, it
727 would have to be assumed that, in contrast to what is observed in other population
728 samples (Karakostis et al., 2017; Karakostis and Lorenzo, 2016), degenerative
729 changes did not only affect the raw size of entheses, but also impacted the proportions
730 among different entheses of each Phaleron individual. Simultaneously, it would also
731 have to be assumed that, especially for the atypical burials (but not the typical ones),
732 these hypothetically age-driven proportions happened to largely coincide with the
733 patterns of documented lifelong manual laborers from a recent sample (of varying
734 biological ages), while also coincidentally reflecting greater thumb extension (i.e.,
735 recruitment of EPB; see Tables 1 and 3). Even though it is impossible to entirely
736 dismiss the above scenario due to the absence of reliable age assessment for most
737 Phaleron individuals, we do not consider it the most parsimonious interpretation of
738 our results.

739 Despite the above differences between atypical and typical burial samples, the
740 results of this study also revealed important similarities. In all PCAs, most individuals
741 of both groups share an overall power-grasping tendency (even if that is
742 systematically higher in most individuals of the atypical burial sample; Figs. 1 and 4
743 to 7). Furthermore, our analyses identified one axis of variance (i.e., PC2 of the
744 second PCA; Fig. 4), which grouped the majority of the Phaleron individuals together

745 in the positive side of the plot, opposite to most values of our modern documented
746 sample from Basel. This difference between the two population samples, which was
747 found to be statistically significant (Table 4), may likely be due to various systemic
748 factors of interpopulation variation in enthesal morphology, such as genes, nutrition,
749 hormones, and age (Foster et al., 2014; Schrader, 2019; Villotte and Knüsel, 2013). In
750 this framework, one could argue that perhaps the unknown effects of these factors
751 may have affected this study's interpretations (e.g., coincidentally leading to the
752 observed overlapping between Basel' lifelong manual workers and Phaleron's
753 atypical burials). However, the Phaleron individuals would still present the observed
754 enthesal patterns (e.g., the one reflecting intense thumb extension in most atypical
755 burials) even without including Basel's lifelong manual laborers in the analyses. That
756 comparison is nevertheless essential for our study's interpretations because it
757 confirms that, in a sample with thorough and long-term occupational documentation,
758 such an enthesal pattern is almost exclusively found in lifelong heavy manual
759 laborers.

760 Even though the methods and results of the present study cannot be used to
761 directly assess population origin, the above enthesal similarities between the two
762 Phaleron groups may be indicative that they both originate from a broadly similar
763 population, at least in terms of general lifestyle and living conditions. This possibility
764 may be also further supported by comparisons among groups in bone pathology and
765 epigenetic traits. Future paleogenetic analysis of the Phaleron skeletons may be able
766 to provide further insights into whether these burial groups represent different
767 populations. Nevertheless, it is worth noting that enthesal variation in our thoroughly
768 documented sample from Basel was not associated with familial relatedness (see
769 Karakostis et al., 2017). Therefore, we would find it unlikely that the same exact PCs

770 (e.g., Fig. 1) representing occupational differences in one population (Basel) would
771 then be driven exclusively by genetic factors in the Phaleron samples.

772 The multivariate results of the present study were consistent between the
773 PCAs combining anatomical sides (Figs. 1 and 4; Table 3) and those performed on
774 each side separately (Figs. 5 to 7; Table 3). Previous research on our documented
775 sample from Basel (also following the V.E.R.A. approach) had also reported similar
776 enthesal correlations between the left and the right side of each individual (see
777 Karakostis et al., 2018). As discussed in that previous research, we believe that such
778 consistency between sides is to be expected for hand enthesal multivariate patterns,
779 regardless of hand preference. This is because a construction worker's preference for
780 using one anatomical side does not negate the fact that heavy manual labor requires
781 bimanual hand use. At the same time, a tailor's precise grasping in one anatomical
782 side does not equate the habitual performance of intense power-grasping in the other.
783 In the comparative framework of a PCA, the signal of intra-individual bilateral
784 differences is likely weaker than the variation across individuals with distinct
785 occupational specializations.

786

787 **5. Conclusions**

788

789 The aim of this study was to provide new insights into the identity of the
790 Phaleron's atypical burials, comparing a general burial sample with a group of
791 apparently executed individuals buried near a major port of Archaic and early
792 Classical Athens. Our results revealed a shared component among most of these
793 individuals, who presented evidence of unusually strenuous manual activities in their

794 hand skeletal remains. Such patterns were present but significantly less distinctive in
795 most of their surrounding burials. Despite the limited sample sizes of this pilot study,
796 its findings comprise a crucial step in creating osteobiographies for these individuals,
797 which will provide a deeper understanding of the socio-political conditions that
798 preceded the rise of Classical Age Athens. We believe that future research could
799 further elucidate the occupational and socioeconomic profiles of the Phaleron burials,
800 hopefully relying on the potential inclusion of additional well-preserved human
801 remains from this cemetery. For instance, extending our research to the muscle
802 attachment sites of other important anatomical regions would likely allow for greater
803 resolution of habitual physical activities. Such data could be further combined with
804 other potential sources of information, involving enthesopathies, osteoarthritis, cross-
805 sectional geometric properties of the long bones, Schmorl's nodes, dental wear,
806 palaeogenetics, and isotopic analyses. Importantly, more nuanced hypotheses on
807 physical activity and socioeconomic status would benefit from a deeper historical
808 investigation of occupational differences in ancient Greece during the historical
809 period in question.

810

811

812 **Acknowledgements**

813

814 We want to thank the excavator Dr. Stella Chryssoulaki and the Ephorate of Piraeus
815 and Islands for the amicable collaboration. Our study and analysis of the human
816 skeletal remains from the cemetery at Phaleron follows the permit issued by the
817 Hellenic Ministry of Culture

818 (ΥΠΟΠΑΙΘ/ΓΔΑΠΚ/ΔΙΠΚΑ/ΤΕΕΑΕΙ158386/93923/8033/777). We are grateful to
819 our funding bodies: the Malcolm Hewitt Wiener Foundation, the Malcolm H. Wiener
820 Laboratory for Archaeological Science of the American School of Classical Studies at
821 Athens, the Paul and Alexandra Canellopoulos Foundation, the School for Human
822 Evolution and Social Change at Arizona State University, the Desnick Family, the
823 National Endowment for the Humanities (Collaborative Research Grant RZ-255623-
824 17), and the National Science Foundation (Senior Archaeology Award BCS-
825 1828645). Special thanks are due to Panagiotis Karkanis, Jim Wright, and Jenifer
826 Neils. The authors are also very grateful to the volunteers of the “Citizen Science
827 Project Basel Spitalfriedhof” (University of Basel, Switzerland) for their hard work on
828 the detailed documentation of our reference sample. Finally, we would like to deeply
829 thank Ioanna Anastopoulou and Giannis Kordonoulis for technical assistance.

830

831 **Data Availability**

832

833 The data that support the findings of this study are available from the corresponding
834 author upon reasonable request.

835

836 **Declaration of competing interests**

837 The authors declare that they have no competing interests.

838

839

840 **References**

- 842 Brooks, S., Suchey, J.M., 1990. Skeletal age determination based on the os pubis: A
843 comparison of the Acsádi-Nemeskéri and Suchey-Brooks methods. *Hum. Evol.* 5,
844 227–238. <https://doi.org/10.1007/BF02437238>
- 845 Bucchi, A., manzanares, M.C., Luengo, J., Bucchi, C., Lorenzo, C., 2019. Muscle strength and
846 enthesal size in human thumbs: testing the relationship with a cadaveric model.
847 *UISPP* 2, 38–42.
- 848 Buikstra, J.E., Ubelaker, D.H., 1994. Standards for data collection from human skeletal
849 remains. Research series no. 44. Arkansas archaeological survey research series no
850 44, Fayetteville.
- 851 Camp, J.M., 2001. *The Archaeology of Athens*. Yale University Press, Yale.
- 852 Cattell, R.B., 1966. The Scree Test For The Number Of Factors. *Multivariate Behavioral*
853 *Research* 1, 245–276.
- 854 Chrysoulaki, S., 2020. The Excavations at Phaleron Cemetery 2012-2017: An Introduction,
855 in: Graml, C., Doronzio, A., Capozzoli, V. (Eds.), *Rethinking Athens before the Persian*
856 *Wars*. Utzverlag, Munich, pp. 103–113.
- 857 Clarkson, H.M., 2000. *Musculoskeletal Assessment: Joint Range of Motion and Manual*
858 *Muscle Strength*. Lippincott Williams & Wilkins, Dallas.
- 859 Corder, G.W., Foreman, D.I., 2014. *Nonparametric Statistics: A Step-by-Step Approach*. John
860 Wiley & Sons, London.
- 861 Davis, C.B., Shuler, K.A., Danforth, M.E., Herndon, K.E., 2013. Patterns of Interobserver Error
862 in the Scoring of Enthesal Changes. *Int. J. Osteoarchaeol.* 23, 147–151.
863 <https://doi.org/10.1002/oa.2277>
- 864 Deymier-Black, A.C., Pasteris, J.D., Genin, G.M., Thomopoulos, S., 2015. Allometry of the
865 Tendon Enthesis: Mechanisms of Load Transfer Between Tendon and Bone. *J.*
866 *Biomech. Eng.* 137, 111005. <https://doi.org/10.1115/1.4031571>
- 867 Edwards, I.E.S., Gadd, C.J., Hammond, N.G.L., Boardman, J., Lewis, D.M., Walbank, F.W.,
868 Astin, A.E., Crook, J.A., Lintott, A.W., Rawson, E., Bowman, A.K., Champlin, E.,
869 Garnsey, P., Rathbone, D., Cameron, A., Ward-Perkins, B., Whitby, M., 1970. *The*
870 *Cambridge Ancient History*. Cambridge University Press, Cambridge.
- 871 Field, A., 2013. *Discovering Statistics Using SPSS, 4th Revised edition*. ed. SAGE Publications
872 Ltd, California.
- 873 Foster, A., Buckley, H., Tayles, N., 2014. Using Enthesis Robusticity to Infer Activity in the
874 Past: A Review. *J Archaeol Method Theory* 21, 511–533.
875 <https://doi.org/10.1007/s10816-012-9156-1>
- 876 Golden, M., 2009. *Greek Sport and Social Status*. University of Texas Press, Texas.
- 877 Hall, J.M., 2007. *A History of the Archaic Greek World: ca. 1200 - 479 BC*. Wiley-Blackwell,
878 London.
- 879 Hartnett, K.M., 2010. Analysis of age-at-death estimation using data from a new, modern
880 autopsy sample--part I: pubic bone. *J. Forensic Sci.* 55, 1145–1151.
881 <https://doi.org/10.1111/j.1556-4029.2010.01399.x>
- 882 Havelková, P., Villotte, S., Velemínský, P., Poláček, L., Dobisíková, M., 2011. Enthesopathies
883 and activity patterns in the Early Medieval Great Moravian population: Evidence of
884 division of labour. *Int. J. Osteoarchaeol.* 21, 487–504.
885 <https://doi.org/10.1002/oa.1164>
- 886 Henderson, C.Y., Mariotti, V., Santos, F., Villotte, S., Wilczak, C.A., 2017. The new Coimbra
887 method for recording enthesal changes and the effect of age-at-death. *B.M.S.A.P.*
888 29, 140–149. <https://doi.org/10.1007/s13219-017-0185-x>
- 889 Holm, S., 1979. A Simple Sequentially Rejective Multiple Test Procedure. *Scandinavian J.*
890 *Stat.* 6, 65–70.

891 Hotz, G., 2017. Theo der Pfeifenraucher – ein genealogisch-naturwissenschaftliches
892 Identifizierungsprojekt. der Schweizerischen Gesellschaft für Familienforschung
893 (SGFF) 44, 29–61.

894 Hotz, G., Steinke, H., 2012. Knochen, Skelette, Krankengeschichten : Spitalfriedhof und
895 Spitalarchiv - zwei sich ergänzende Quellen. Basl. Z. Gesch. Altertumskd. Bd. 112,
896 105–138.

897 Ingvarsson-Sundström, A., Backstrom, Y., 2019. Bioarchaeological field analysis of human
898 remains from the mass graves at Phaleron, Greece : With an introduction by Stella
899 Chryssoulaki and an appendix by Anna Linderholm, Anna Kjellstrom, Vendela Kempe
900 Lagerholm, and Maja Krzewirska. Swedish Institute of Athens and Rome, Stockholm.

901 Jorgensen, K.C., Mallon, L., Kranioti, E.F., 2020. Testing interobserver and intraobserver
902 agreement of the original and revised Coimbra Methods. *Int. J. Osteoarchaeol.* 30,
903 769–777. <https://doi.org/10.1002/oa.2907>

904 Karakostis, F.A., Harvati, K., 2021. New horizons in reconstructing past human behavior:
905 Introducing the “Tübingen University Validated Entheses-based Reconstruction of
906 Activity” method. *Evol. Anthropol.* <https://doi.org/10.1002/evan.21892>.
907 <https://doi.org/10.1002/evan.21892>

908 Karakostis, F.A., Hotz, G., Scherf, H., Wahl, J., Harvati, K., 2018a. A repeatable geometric
909 morphometric approach to the analysis of hand enthesal three-dimensional form.
910 *Am. J. Phys. Anthropol.* 166, 246–260. <https://doi.org/10.1002/ajpa.23421>

911 Karakostis, F.A., Hotz, G., Scherf, H., Wahl, J., Harvati, K., 2017. Occupational manual activity
912 is reflected on the patterns among hand entheses. *Am. J. Phys. Anthropol.* 164, 30–
913 40. <https://doi.org/10.1002/ajpa.23253>

914 Karakostis, F.A., Hotz, G., Tourloukis, V., Harvati, K., 2018b. Evidence for precision grasping in
915 Neandertal daily activities. *Sci. Adv.* 4, eaat2369.
916 <https://doi.org/10.1126/sciadv.aat2369>

917 Karakostis, F.A., Jeffery, N., Harvati, K., 2019a. Experimental proof that multivariate patterns
918 among muscle attachments (entheses) can reflect repetitive muscle use. *Sci. Rep.* 9,
919 1–9. <https://doi.org/10.1038/s41598-019-53021-8>

920 Karakostis, F.A., Lorenzo, C., 2016. Morphometric patterns among the 3D surface areas of
921 human hand entheses. *Am. J. Phys. Anthropol.* 160, 694–707.
922 <https://doi.org/10.1002/ajpa.22999>

923 Karakostis, F.A., Reyes-Centeno, H., Francken, M., Hotz, G., Rademaker, K., Harvati, K., 2020.
924 Biocultural evidence of precise manual activities in an Early Holocene individual of
925 the high-altitude Peruvian Andes. *Am. J. Phys. Anthropol.*
926 <https://doi.org/10.1002/ajpa.24160>. <https://doi.org/10.1002/ajpa.24160>

927 Karakostis, F.A., Vlachodimitropoulos, D., Piagkou, M., Scherf, H., Harvati, K., Moraitis, K.,
928 2019c. Is Bone Elevation in Hand Muscle Attachments Associated with
929 Biomechanical Stress? A Histological Approach to an Anthropological Question.
930 *Anat. Rec.* 302, 1093–1103. <https://doi.org/10.1002/ar.23984>

931 Karakostis, F.A., Wallace, I.J., Konow, N., Harvati, K., 2019b. Experimental evidence that
932 physical activity affects the multivariate associations among muscle attachments
933 (entheses). *J. Exp. Biol.* 222, 213058. <https://doi.org/10.1242/jeb.213058>

934 Keramopoulos, A.D., 1923. O apotypanismos: symvoli archaiologiki eis tin istorian tou
935 poinikou dikaiou kai tin laografian. Estia, Athens.

936 Klales, A.R., Ousley, S.D., Vollner, J.M., 2012. A revised method of sexing the human
937 innominate using Phenice’s nonmetric traits and statistical methods. *Am. J. Phys.*
938 *Anthropol.* 149, 104–114. <https://doi.org/10.1002/ajpa.22102>

939 Lagia, A., 2000. Kerameikos Grabung 1999. Preliminary Analysis of the Human Skeletal
940 Remains. *Archäologischer Anzeiger* 481–483.

- 941 Larsen, C.S., 1999. *Bioarchaeology: Interpreting Behavior from the Human Skeleton*.
942 Cambridge University Press, Cambridge.
- 943 Mariotti, V., Facchini, F., Belcastro, M.G., 2004. Enthesopathies--proposal of a standardized
944 scoring method and applications. *Coll. Antropol.* 28, 145–159.
- 945 Mariotti, V., Facchini, F., Giovanna Belcastro, M., 2007. The study of entheses: proposal of a
946 standardised scoring method for twenty-three entheses of the postcranial skeleton.
947 *Coll. Antropol.* 31, 291–313.
- 948 Marzke, M.W., Toth, N., Schick, K., Reece, S., Steinberg, B., Hunt, K., Linscheid, R.L., An, K.-N.,
949 1998. EMG study of hand muscle recruitment during hard hammer percussion
950 manufacture of Oldowan tools. *Am. J. Phys. Anthropol.* 105, 315–332.
- 951 Merritt, C.E., 2015. The influence of body size on adult skeletal age estimation methods. *Am.*
952 *J. Phys. Anthropol.* 156, 35–57. <https://doi.org/10.1002/ajpa.22626>
- 953 Michopoulou, E., Nikita, E., Henderson, C.Y., 2017. A Test of the Effectiveness of the Coimbra
954 Method in Capturing Activity-induced Enthesal Changes. *Int. J. Osteoarchaeol.* 27,
955 409–417. <https://doi.org/10.1002/oa.2564>
- 956 Milner, G., Boldsen, J., 2016. *Transition Analysis Age Estimation Skeletal Scoring Manual*.
957 *Fordisc Version 1.02*. Forensic Anthropology Center, University of Tennessee,
958 Knoxville.
- 959 Morris, I., 2009. The Eighth-Century Revolution, in: *A Companion to Archaic Greece*. John
960 Wiley & Sons, Ltd, pp. 64–80. <https://doi.org/10.1002/9781444308761.ch4>
- 961 Nicholson, N.J., 2011. *Aristocracy and Athletics in Archaic and Classical Greece*, Reissue
962 Edition. ed. Cambridge University Press, Cambridge.
- 963 Nikita, E., Xanthopoulou, P., Bertatos, A., Chovalopoulou, M.-E., Hafez, I., 2019. A three-
964 dimensional digital microscopic investigation of enthesal changes as skeletal
965 activity markers. *Am. J. Phys. Anthropol.* 169, 704–713.
966 <https://doi.org/10.1002/ajpa.23850>
- 967 Noldner, L.K., Edgar, H.J.H., 2013. Technical note: 3D representation and analysis of entheses
968 morphology. *Am. J. Phys. Anthropol.* 152, 417–424.
969 <https://doi.org/10.1002/ajpa.22367>
- 970 Nolte, M., Wilczak, C., 2013. Three-dimensional Surface Area of the Distal Biceps Enthesis,
971 Relationship to Body Size, Sex, Age and Secular Changes in a 20th Century American
972 Sample. *Int. J. Osteoarchaeol.* 23, 163–174. <https://doi.org/10.1002/oa.2292>
- 973 Osborne, R., 2009. *Greece in the Making 1200-479 BC*. Routledge, London.
- 974 Pearson, O.M., Lieberman, D.E., 2004. The aging of Wolff's "law": ontogeny and responses to
975 mechanical loading in cortical bone. *Am. J. Phys. Anthropol. Suppl* 39, 63–99.
976 <https://doi.org/10.1002/ajpa.20155>
- 977 Pelekidis, S., 1916. Excavations at Phaleron. *Archaeologikon Deltion* 2, 13–64.
- 978 Phenice, T.W., 1969. A newly developed visual method of sexing the os pubis. *Am. J. Phys.*
979 *Anthropol.* 30, 297–301. <https://doi.org/10.1002/ajpa.1330300214>
- 980 Prevedorou, E.-A., Buikstra, J.E., 2019. Bioarchaeological Practice and the Curation of Human
981 Skeletal Remains in a Greek Context: The Phaleron Cemetery. *Adv. Archaeol.*
982 *Practice* 7, 60–67. <https://doi.org/10.1017/aap.2018.42>
- 983 Pritchard, D.M., 2012. *Sport, Democracy and War in Classical Athens*. Cambridge University
984 Press, Cambridge. <https://doi.org/10.1017/CBO9781139030519>
- 985 Schrader, S., 2019. *Activity, Diet and Social Practice: Addressing Everyday Life in Human*
986 *Skeletal Remains, Bioarchaeology and Social Theory*. Springer International
987 Publishing, New York. <https://doi.org/10.1007/978-3-030-02544-1>
- 988 Villotte, S., 2006. Connaissances médicales actuelles, cotation des enthésopathies : nouvelle
989 méthode. *B.M.S.A.P.* 18, 65–85.

990 Villotte, S., Castex, D., Couallier, V., Dutour, O., Knüsel, C.J., Henry-Gambier, D., 2010.
991 Enthesopathies as occupational stress markers: evidence from the upper limb. *Am. J.*
992 *Phys. Anthropol.* 142, 224–234. <https://doi.org/10.1002/ajpa.21217>
993 Villotte, S., Knüsel, C.J., 2014. “I sing of arms and of a man...”: medial epicondylitis and the
994 sexual division of labour in prehistoric Europe. *J. Archaeol. Sci.* 43, 168–174.
995 <https://doi.org/10.1016/j.jas.2013.12.009>
996 Villotte, S., Knüsel, C.J., 2013. Understanding Enteseal Changes: Definition and Life Course
997 Changes. *Int. J. Osteoarchaeol.* 23, 135–146. <https://doi.org/10.1002/oa.2289>
998 Walker, P.L., 2008. Sexing skulls using discriminant function analysis of visually assessed
999 traits. *Am. J. Phys. Anthropol.* 136, 39–50. <https://doi.org/10.1002/ajpa.20776>
1000 Walker, P.L., 2005. Greater sciatic notch morphology: Sex, age, and population differences.
1001 *Am. J. Phys. Anthropol.* 127, 385–391. <https://doi.org/10.1002/ajpa.10422>
1002 Wallace, I.J., Winchester, J.M., Su, A., Boyer, D.M., Konow, N., 2017. Physical activity alters
1003 limb bone structure but not enteseal morphology. *J. Hum. Evol.* 107, 14–18.
1004 <https://doi.org/10.1016/j.jhevol.2017.02.001>
1005 Wilczak, C., Mariotti, V., Pany-Kucera, D., Villotte, S., Henderson, C., 2016. Training and
1006 Interobserver Reliability in Qualitative Scoring of Skeletal Samples. *J. Archaeol. Sci.*
1007 *Rep.* 11, 69–79. <https://doi.org/10.1016/j.jasrep.2016.11.033>
1008 Williams-Hatala, E.M., Hatala, K.G., Hiles, S., Rabey, K.N., 2016. Morphology of muscle
1009 attachment sites in the modern human hand does not reflect muscle architecture.
1010 *Sci. Rep.* 6, 1–8. <https://doi.org/10.1038/srep28353>
1011 Zumwalt, A., 2006. The effect of endurance exercise on the morphology of muscle
1012 attachment sites. *J. Exp. Biol.* 209, 444–454. <https://doi.org/10.1242/jeb.02028>
1013

Declaration of interests

The authors declare that they have no known competing financial interests or personal relationships that could have appeared to influence the work reported in this paper.

The authors declare the following financial interests/personal relationships which may be considered as potential competing interests: